

# Detailed experimental and kinetic modeling study of cyclopentadiene pyrolysis in the presence of ethene

*Alexander J. Vervust<sup>a</sup>, Marko R. Djokic<sup>a</sup>, Shamel S. Merchant<sup>b</sup>, Hans-Heinrich Carstensen<sup>a</sup>,  
Alan E. Long<sup>c</sup>, Guy B. Marin<sup>a</sup>, William H. Green<sup>c</sup>, Kevin M. Van Geem<sup>a</sup>✉*

a) Laboratory for Chemical Technology, Ghent University, Technologiepark 914, B-9052 Gent,  
Belgium

b) ExxonMobil Research and Engineering, 1545 Route US 22 East, Annandale, N.J. 08801, USA

c) Department of Chemical Engineering, Massachusetts Institute of Technology, 77  
Massachusetts Ave., Cambridge, MA 02139, USA

✉ corresponding author. E-mail: Kevin.VanGeem@UGent.be

## Supporting Information

## 1. Experimental

### 1.1 Pyrolysis setup

Figure S1 shows a schematic overview of the bench-scale pyrolysis setup. Three main sections can be distinguished: the feed section, the reactor/furnace section and the product analysis section<sup>1-5</sup>.

Dicyclopentadiene (DCPD) (Sigma-Aldrich, 99+% purity) was used as cyclopentadiene (CPD) source. The DCPD purity was confirmed to be 99+% using a GC×GC-FID setup. The composition of the DCPD is presented in Table S1. DCPD is present as its endo-DCPD and exo-DCPD isomers. Even though the exo isomer is thermodynamically more stable, the DCPD used for this study contains mostly the endo isomer as it forms much faster than the exo isomer, typical for commercial grade DCPD. The CPD, present in the chromatogram, was produced by the degradation of its dimer DCPD during the hot-needle injection. The main impurities of the DCPD are C<sub>10</sub>H<sub>14</sub> (hydrogenated DCPD) and C<sub>11</sub>H<sub>14</sub> polycyclic compounds.

Prior to entering the reaction section, the DCPD molecules will undergo a retro-Diels Alder reaction in the evaporation and mixing section producing 2 CPD molecules. The latter implies that purity of CPD at the inlet of the reactor is 99.7 mol% assuming the impurities do not decompose. This has been confirmed by performing a test at a temperature of 673K along the entire reactor, which is low enough to prevent any reaction from occurring. The results of the effluent analysis using GC×GC-FID/TOF-MS are shown in Table S2. As expected the DCPD decomposes to CPD with a purity of 99.7 mol%.

The DCPD is melted (307 K) and fed to an evaporator kept at 473 K using a coriolis flow meter controlled pump (Bronkhorst, The Netherlands). The temperature in the evaporator is 20 K

above the boiling point of DCPD (453 K), which is sufficient to gasify DCPD and completely convert it into CPD in-line with the work of Kim et al.<sup>6</sup>. The co-reactant ethene (Air Liquide, Belgium, 99.5% purity) is mixed with the diluent N<sub>2</sub> (Air Liquide, Belgium, purity 99.999%, less than 2 and 3 ppm-mol of O<sub>2</sub> and H<sub>2</sub>O respectively) and heated separate from the DCPD to the same temperature. The evaporators/heaters and mixer are electrically heated and filled with quartz beads to enable a smooth evaporation of the DCPD and a uniform mixing of the feed and diluent. The flow rates of ethene and diluent are controlled by coriolis mass flow controllers (Bronkhorst, The Netherlands). A dilution of 1 mol CPD / 1 mol ethene / 10 mol N<sub>2</sub> was used for the experiments discussed here, while temperature ranged from 873 to 1163 K. Information on the experimental conditions can be found in Table S3. Flow rates were chosen to obtain CPD conversions ranging from a few percent up to 92%, correspond to a space time between 300 to 400 ms. While changing the reactor temperature profile the mass flows were kept constant, which resulted in slightly varying residence times with reactor temperature.

The reactor is a 1.475 m long tube with an internal diameter of 6 mm, made of Incoloy 800HT (Ni, 30-35; Cr, 19-23; and Fe, >39.5 wt %). The reactor is placed vertically in a rectangular furnace which is heated electrically. The reactor is operated nearly isothermally, i.e. the temperature increases steeply at the inlet and drops steeply at the outlet of the reactor (see Figure S8). Thermocouples (type K) are used to monitor the process gas temperature at eight axial positions (see Figure S1). The thermocouple manufacturers adhere to the specifications for calibration accuracy (limits of error) of the American Society for Testing Materials (ASTM) for type K thermocouples, namely 0-1250°C (32-2300°F): ±2.2°C or 0.75% of reading in °C, whichever is greater<sup>7</sup>. The reactor pressure is controlled by an outlet pressure restriction valve. The coil inlet pressure (CIP) and coil outlet pressure (COP) are measured by two manometers,

situated at the inlet and outlet of the reactor, respectively. The pressure drop over the reactor was found to be negligible. The pressure in the reactor remained constant at 1.7 bara.

The significance of the catalytic activity of the reactor wall has been tested by repeating a number of CPD pyrolysis experiments in an 8 mm internal diameter reactor, resulting in a 24% lower surface-to-volume (S/V) ratio both with CPD and JP-10 (note that CPD is one of the main decomposition products of JP-10).<sup>8</sup> If the wall/coke layer has a significant activity, a different S/V ratio would lead to different conversions and product distribution, given that all other reaction and operating conditions remain the same. The properties of both reactors are given in Table S4. The operating conditions in both reactors were kept identical, i.e. the same COP of 1.7 bara and identical temperature profiles. The hydrocarbon flow rate is increased in the reactor with larger diameter to obtain the same space time. The diluent flow rate is increased proportionally to obtain the same dilution. Experiments with both reactor configurations were performed on consecutive days. Differences in conversion and product distributions between the 6 mm and 8 mm ID reactor for the pyrolysis of CPD and JP-10 remain within the experimental error of 5% rel, providing proof that wall effects can be neglected.

## 1.2 Product analysis

The analysis section of the pyrolysis set-up enables the on-line identification and quantification of the entire product stream.<sup>3-5</sup> It contains two different gas chromatographs: a refinery gas analyzer (RGA) and a GC×GC-FID/TOF-MS setup (Thermo Scientific, Interscience Belgium); see Figure S1. A representation of the used GCs and reference components is given in Figure S2. An overview of the GC×GC-FID/TOF-MS settings used in this work can be found in Table S5.

The reactor effluent enters a heated sampling system consisting of two high temperature 6-way port 2-way valves, kept at 575 K to prevent condensation of high molecular weight components. The temperature at which sampling occurs is well above the dew point of the effluent, as shown by Van Geem et al.<sup>9</sup>. The valve-based sampling manifold (see Figure S3) and uniformly heated transfer lines are used to inject a gaseous sample of the reactor effluent into the GC×GC, which is equipped with a FID and a TEMPUS TOF-MS (Thermo Scientific, Interscience Belgium), enabling both qualitative and quantitative analyses of the entire product stream, from methane to PAHs<sup>3, 5</sup>. The reactor effluent is cooled to 323 K further downstream using a water-cooled heat exchanger. The condensed products are collected in a liquid separator and the remainder of the effluent stream is sent to the vent. A fraction of the effluent is automatically injected into the RGA, before reaching the vent, using built-in gas sampling valves (353 K). This analysis allows the detection of all permanent gasses, such as N<sub>2</sub> and H<sub>2</sub>, present in the effluent, as well as an additional analysis of the light hydrocarbons, i.e. C<sub>1</sub> – C<sub>4</sub>.

Aside from being a diluent, N<sub>2</sub> also serves as the primary internal standard for the determination of the absolute flow rates of the components in the reactor effluent. Flow rates of H<sub>2</sub>, CH<sub>4</sub>, CO<sub>2</sub> and C<sub>2</sub> hydrocarbons are calculated using the peak areas of the RGA TCD, the experimentally determined relative (to methane) response factors for this instrument, and the known amount of nitrogen added in the reactor feed. The equation below shows how the CH<sub>4</sub> mass flow rate in the reactor effluent can be determined based on the known N<sub>2</sub> mass flow rate, peak areas and relative response factors:

$$\dot{m}_{CH_4} = \frac{f_{CH_4} \cdot A_{CH_4}}{f_{N_2} \cdot A_{N_2}} \cdot \dot{m}_{N_2}$$

Note that the response factor of methane is chosen arbitrary to be unity ( $f_{CH_4} = 1$ ). Based on the calculated absolute mass flow rates weight fraction (%) of the detected compounds in the effluent can be calculated using the following equation:

$$y_i = \frac{\dot{m}_i}{\dot{m}_0} \cdot 100 (\%)$$

where  $y_i$  is the yield of compound  $i$ ,  $\dot{m}_i$  is the mass flow rate of component  $i$  in effluent,  $\dot{m}_0$  is the mass flow rate of the hydrocarbon feed.

To quantify the peaks of the hydrocarbons with higher molecular masses on the flame ionization channel of the RGA and GC×GC-FID methane is used as a secondary internal standard. Peak integration of the chromatograms obtained from GC×GC is performed by a commercial integration package, GC-Image (Zoex Corp.). Component identification is accomplished using two independent orthogonal parameters: the Kovats retention indices and the associated mass spectra obtained from GC×GC-TOF-MS analyses. Response factors of the permanent gasses (H<sub>2</sub>, CH<sub>4</sub>) and light hydrocarbons (C<sub>1</sub>-C<sub>4</sub>) have been determined by means of a gaseous calibration mixture (Air Liquide, Belgium). The response factors of all C<sub>5+</sub> hydrocarbons were determined using the carbon number concept, relative to methane<sup>10</sup>. At each studied temperature at least 3 repeat analyses were performed with the RGA which takes about one third of the time necessary to complete one GC×GC analysis. Deviations in the obtained results are attributed to uncertainties on the mass flow rates of both feed (CPD, ethene) and the internal standard (N<sub>2</sub>). Replicate experiments were performed for two different temperatures to calculate the experimental error on the obtained results, which was less than 10% for all detected results, with 9% for naphthalene being the highest. The mass balances closed within 5%. All component weight fractions were normalized to sum up to 100 wt%, enabling the straight

forward interpretations of the results. The molar C to H ratio of 0.7 mol C / mol H in the feed was well conserved in the reactor effluent, with a maximum deviation of 1.6% at 1073 K.

## Tables

Table S1. Feedstock (DCPD) composition determined using GC×GC-FID.

Compound Name	wt%	type	#C	#H
<b>1,3-cyclopentadiene</b>	0.05	naphthenic	5	6
C <sub>10</sub> H <sub>14</sub>	0.26	polycyclic	10	14
<b>exo-dicyclopentadiene</b>	1.36	polycyclic	10	12
<b>endo-dicyclopentadiene</b>	97.88	polycyclic	10	12
C <sub>11</sub> H <sub>14</sub>	0.42	polycyclic	11	14
C <sub>11</sub> +	0.03	aromatic	-	-

Table S2. Unreacted feedstock (CPD) composition determined using GC×GC-FID.

Compound Name	wt%	mol%	type
1,3-cyclopentadiene	99.42	99.73	naphthenic
C <sub>10</sub> +	0.58	0.27	polycyclic

Table S3. Detailed information about product spectra detected during CPD-ethene co-pyrolysis, including temperature profiles in the reaction zone and feed flow rates.

Conditions							
Feed							
CPD [g/h]	49	49	49	49	49	49	49
Ethene [g/h]	21	21	21	21	21	21	21



N2 Dilution [g/h]	206	206	206	206	206	206	206
Feed,[mol/h]							
CPD [mol/h]	0.74	0.74	0.74	0.74	0.74	0.74	0.74
Ethene [mol/h]	0.75	0.75	0.75	0.75	0.75	0.75	0.75
N2 Dilution [mol/h]	7.4	7.4	7.4	7.4	7.4	7.4	7.4
Dilution, molN2/molHC	5	5	5	5	5	5	5
T-profile reactor [K]							
CIT	740.1	768.8	798.0	820.9	843.5	873.7	887.3
T at 190 mm	873.4	924.0	974.1	1023.7	1073.0	1125.5	1166.9
T at 380 mm	895.2	947.6	997.8	1049.9	1102.4	1154.5	1200.5
T at 480 mm	872.7	922.9	973.1	1022.3	1072.7	1122.9	1164.1
T at 670 mm	857.8	908.4	959.8	1008.4	1057.8	1114.4	1154.4
T at 860 mm	873.2	923.8	973.6	1023.2	1073.4	1124.7	1165.9
T at 1050 mm	876.5	926.9	976.5	1026.6	1077.2	1130.0	1172.2
T at 1240 mm	873.8	924.2	974.6	1024.3	1075.4	1126.3	1167.8
T at 1430 mm	760.8	808.1	851.7	901.2	950.8	909.2	946.4
COT at 1475 mm	721.7	722.1	721.9	721.8	722.1	723.2	723.2
Tsetting [K]	873	923	973	1023	1073	1123	1163
P-profile reactor [MPa]							

CIP	0.17	0.17	0.17	0.17	0.17	0.17	0.17
COP	0.17	0.17	0.17	0.17	0.17	0.17	0.17
Compound name	wt %						
hydrogen	0.00	0.01	0.02	0.09	0.20	0.69	1.19
methane	0.00	0.02	0.11	0.36	1.13	2.97	4.09
ethylene	29.92	29.81	29.50	29.08	29.14	26.61	24.50
ethane	0.00	0.02	0.08	0.27	0.38	0.69	0.43
propylene	0.00	0.04	0.05	0.16	0.35	0.82	0.79
1,3-butadiene	0.00	0.00	0.02	0.09	0.40	0.66	0.79
1,3-cyclopentadiene	69.16	68.76	66.47	59.09	43.57	19.88	5.35
cyclopentene	0.16	0.30	0.42	0.56	0.30	0.10	0.08
fulvene	0.00	0.00	0.03	0.08	0.05	0.06	0.06
5-methyl-1,3-cyclopentadiene	0.01	0.01	0.07	0.31	0.27	0.15	0.09
1-methyl-1,3-cyclopentadiene	0.00	0.01	0.06	0.26	0.24	0.13	0.08
benzene	0.01	0.03	0.21	1.16	2.77	8.56	11.68
1,3-cyclohexadiene	0.00	0.00	0.03	0.08	0.07	0.05	0.04
2-Norbonene (C7H10-1)	0.07	0.05	0.05	0.05	0.02	0.24	0.13
C7H10-2	0.10	0.10	0.19	0.14	0.04	0.03	0.07
C7H10-3	0.07	0.08	0.15	0.18	0.04	0.03	0.05
toluene	0.02	0.00	0.03	0.18	0.43	1.98	3.74
C7H8	0.00	0.00	0.03	0.04	0.05	0.06	0.06
ethylbenzene	0.00	0.00	0.00	0.00	0.00	0.03	0.12

xylene (m, p)	0.00	0.00	0.00	0.00	0.01	0.08	0.28
phenylethyne	0.00	0.00	0.00	0.00	0.00	0.04	0.27
o-xylene	0.00	0.00	0.00	0.00	0.01	0.04	0.13
styrene	0.00	0.00	0.01	0.00	0.17	0.92	2.43
C9H10	0.00	0.00	0.01	0.00	0.03	0.23	0.66
indane	0.00	0.00	0.00	0.01	0.03	0.05	0.11
indene	0.03	0.08	0.56	2.03	4.82	7.63	5.95
C10H12 aromatics	0.13	0.06	0.08	0.02	0.09	0.10	0.08
methyl-indenes	0.24	0.34	0.90	1.58	2.27	1.34	0.47
1,2-dihydro-Naphthalene	0.03	0.10	0.41	1.29	1.45	0.42	0.29
naphthalene	0.05	0.09	0.40	2.33	7.19	16.74	20.44
C10H10	0.00	0.08	0.09	0.10	0.04	0.04	0.01
C11H10 diaromatics	0.00	0.00	0.00	0.00	0.11	0.33	0.49
2-methyl-Naphthalene	0.00	0.00	0.00	0.01	0.08	0.29	0.62
1-methyl-naphthalene	0.00	0.00	0.00	0.00	0.03	0.34	0.57
C10H8-1	0.00	0.00	0.00	0.02	0.03	0.02	0.02
acenaphthylene	0.00	0.00	0.01	0.06	0.30	0.73	1.63
C12H10	0.00	0.00	0.00	0.05	0.09	0.53	1.29
Fluorene	0.00	0.00	0.00	0.00	0.19	0.64	1.29
C13H10 naphthenodiaromatics	0.00	0.00	0.00	0.03	0.44	0.63	0.98
C14H12 naphthenodiaromatics	0.00	0.00	0.00	0.03	0.78	0.92	1.17
phenanthrene	0.00	0.00	0.00	0.02	0.44	1.29	2.35
anthracene	0.00	0.00	0.00	0.03	0.37	0.81	1.39
C15H14	0.00	0.00	0.00	0.00	0.02	0.07	0.12

naphthenodiaromatics							
C15H12 naphthenodiaromatics	0.00	0.00	0.00	0.09	0.24	0.46	0.60
C15H10 naphthenotriaromatics	0.00	0.00	0.00	0.05	0.63	0.41	0.57
C16H12 naphthenodiaromatics	0.00	0.00	0.00	0.00	0.02	0.05	0.15
Fluoranthene	0.00	0.00	0.00	0.00	0.05	0.09	0.30
C16H12 triaromatics	0.00	0.00	0.00	0.05	0.14	0.19	0.71
C16H10 naphthenotriaromatics	0.00	0.00	0.00	0.00	0.07	0.10	0.19
pyrene	0.00	0.00	0.00	0.00	0.02	0.05	0.14
C17H12 naphthenotriaromatics	0.00	0.00	0.00	0.00	0.11	0.23	0.44
C1 pyrenes	0.00	0.00	0.00	0.00	0.02	0.05	0.09
C18H12 tetraaromatics	0.00	0.00	0.00	0.00	0.18	0.27	0.29
C18H14	0.00	0.00	0.00	0.00	0.00	0.00	0.00
C19H14 tetraaromatics	0.00	0.00	0.00	0.00	0.07	0.11	0.14
Sum *	100.00	100.00	100.00	100.00	100.00	100.00	100.00

\* All component weight fractions were normalized to sum up to 100 wt%

Table S4. Properties and dimensions of used reactors to provide proof that wall effects can be neglected.

	6mm ID Reactor	8mm ID reactor
Reactor material	Incoloy 800HT	Incoloy 800HT
Reactor diameter (ID) / mm	6	8
Reactor length / m	1.475	1.475

Surface-to-volume ratio / mm <sup>-1</sup>	0.66	0.5
CPD or JP-10 mass flow rate / (10 <sup>-2</sup> g s <sup>-1</sup> )	2.33	4.14
N <sub>2</sub> mass flow rate / (10 <sup>-2</sup> g s <sup>-1</sup> )	4.67	8.30

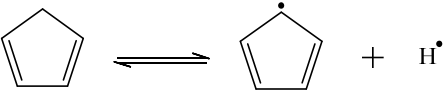
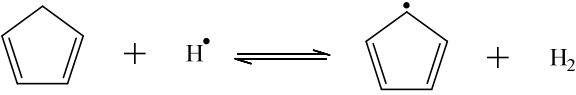
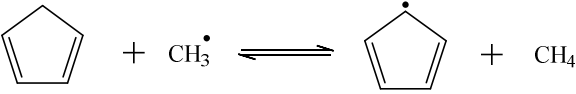
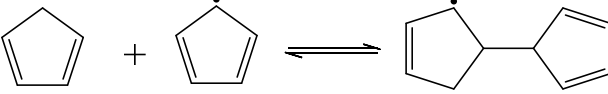
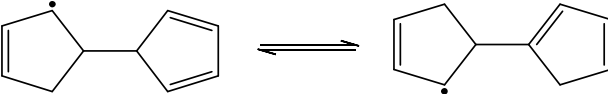
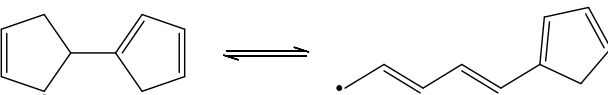
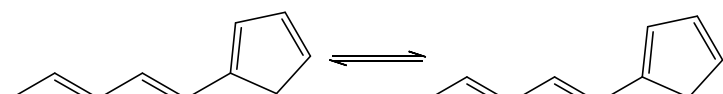
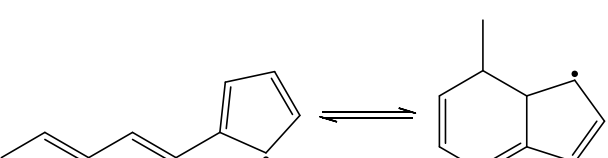
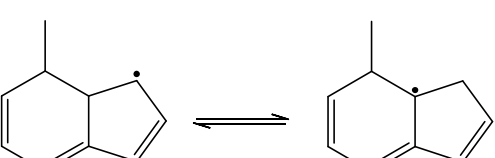
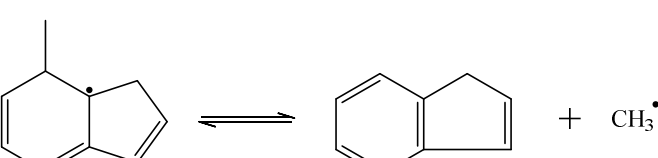
Table S5. GC × GC settings for on-line effluent analysis

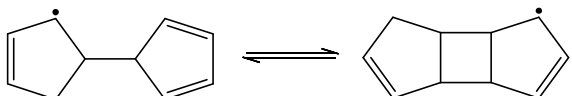
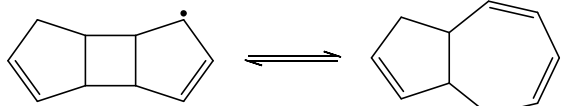
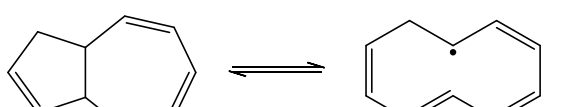
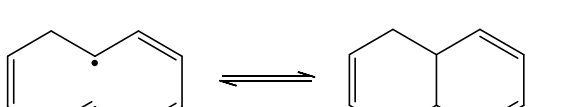
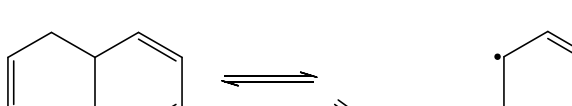
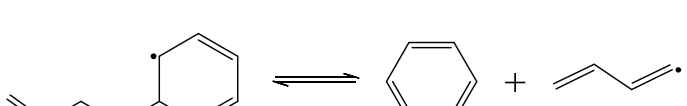
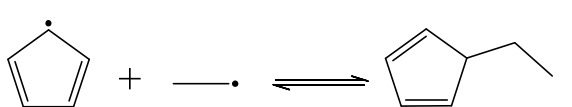
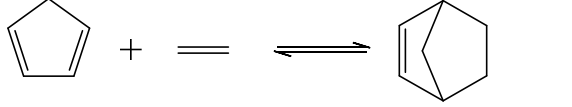
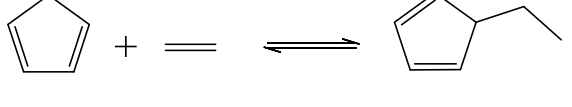
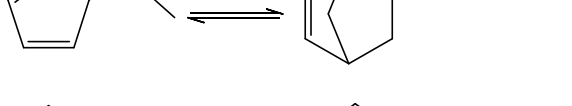
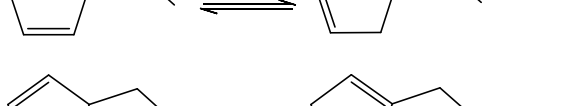

Detector	FID, 300°C	TOF-MS, 25-350 amu
Injections (SSL)	Gas injection, split flow 50 ml/min, 280°C	
First column	RTX-1 PONA or MXT-1 <sup>a</sup> 60 m L × 0.25 mm I.D. × 0.25 μm df	
Second column	BPX-50 <sup>b</sup> 2 m L × 0.15 mm I.D. × 0.15 μm df	
Oven temperature	-40°C (4 min hold) → 40°C at 5°C/min → 370°C (for MXT-1; 300°C for RTX-1) at 4°C/min	
Modulation Period	5 s (cryogenic CO <sub>2</sub> )	
Carrier gas	He, constant flow 2.1 ml/min	He, constant flow 3.5 ml/min

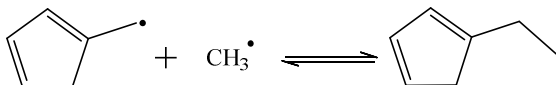
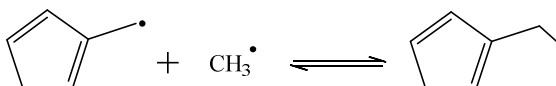
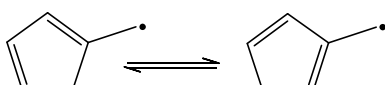
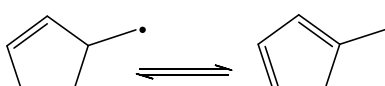


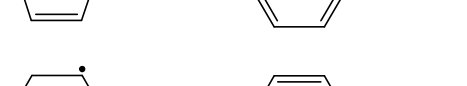
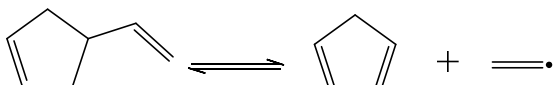
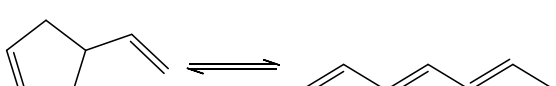
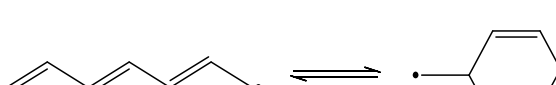


<sup>a</sup> dimethyl polysiloxane (*Restek*); <sup>b</sup> 50% phenyl polysilphenylene-siloxane (*SGE*)

Table S6. Arrhenius parameters for the dominant reactions for the formation of the primary aromatic products during cyclopentadiene pyrolysis. The parameters are given in units of s<sup>-1</sup>, cm<sup>3</sup>, mol<sup>-1</sup> and kcal.

Reaction	A	n	E <sub>a</sub>	Ref
<i>Cyclopentadienyl</i>				

	5.2E+14	0	0	<sup>11</sup> × 2
	5.1E+07	1.9	4.0	a
	6.1E+02	2.9	5.0	a
<i>Naphthalene</i>				
The pressure dependent rate expressions, determined by Long et al. <sup>12</sup> for the formation pathways of naphthalene have been used.				
<i>Indene</i>				
	2.83E+02	2.74	3.3	a
	1.12E+08	1.64	22.7	a
	1.91E+10	1.04	31.2	a
	2.59E+08	1.01	26.4	a
	7.9E+10	0.29	21.1	a
	6.07E+06	2.0	26.1	a
	1.71E+11	0.86	22.7	a

Benzene					
	1.89E+11	0.29	15.4	a	
	3.5E+13	0.58	29.1	a	
	1.68E+12	0.91	36.4	a	
	6.25E+09	0.76	6.2	a	
	8.76E+10	0.78	24.5	a	
	7.14E+12	0.52	22.9	a	
	1.0E+13	0	0	b	
	2.0E+10	0	24.7	b	
	1.94E-01	3.47	25.6	a	
	6.0E+10	0	5.0	b	
	1.01E+08	1.74	24.3	b	
	1.01E+08	1.74	24.3	b	

	1.02E+14	-0.32	-0.13	b
	1.02E+14	-0.32	-0.13	b
	9.22E+03	2.81	30.2	a
	2.23E+07	1.54	13.4	a
	3.18E+11	0.17	4.4	a
	8.51E+11	0.41	16.7	a
	1.84E+09	1.3	27.4	a
<i>Toluene</i>				
	1.89E+12	0.87	45.0	a
	2.77E+10	0.87	35.0	a
	3.95E+10	0.53	31.5	a
	1.72E+07	1.81	23.3	a
	1.06E+10	1.26	28.1	a
<i>Styrene</i>				



	$1.0\text{E}+13$	0	0	b
	$8.78\text{E}+07$	1.58	21.7	b
	$8.78\text{E}+07$	1.58	21.7	b
	$4.24\text{E}+13$	0	21.7	b
	$4.24\text{E}+13$	0	21.7	b
	$2.01\text{E}+14$	0	6.2	b
	$2.01\text{E}+14$	0	6.2	b
	$1.31\text{E}+13$	0	9.9	b
	$1.31\text{E}+13$	0	9.9	b
	$8.78\text{E}+07$	1.58	21.7	b
	$8.78\text{E}+07$	1.58	21.7	b
	$6.62\text{E}+12$	0.21	14.0	b
	$3.31\text{E}+12$	0.21	16.6	b
	$8.81\text{E}+06$	1.95	5.9	b

a: These kinetic parameters had been calculated using the CBS-QB3 method as part of this work and have been made available in the RMG database; b: Kinetic parameters determined by RMG rate rules.

Table S7. Naphthalene, fulvalene and azulene yields predicted by the kinetic model at the conditions of the low and high dilution CPD experiments of Djokic et al.<sup>8</sup> and the CPD/ethene co-pyrolysis experiments performed as part of this work.

		Naphthalene		Fulvalene		Azulene
	CPD conversion [wt%]	Yield [wt%]		Yield [wt%] Ratio fulvalene to naphthalene [%]	Yield [wt%]	Ratio azulene to naphthalene [%]
<b>CPD (1 mol CPD / 5 mol N<sub>2</sub>)</b>						
973 K	6.2	0.15	0.005	3.2	0.014	8.9
1023 K	25.8	1.99	0.038	1.9	0.17	8.8
1073 K	59.7	13.24	0.058	0.4	0.60	4.5
1123 K	86.9	38.72	0.031	0.1	0.46	1.2
<b>CPD (1 mol CPD / 24 mol N<sub>2</sub>)</b>						
973 K	3.4	0.05	1.4E-03	2.8	4.6E-03	8.9
1023 K	14.3	0.78	0.011	1.5	0.08	10.2
1073 K	39.6	7.68	0.032	0.4	0.54	7.0
1123 K	69.8	29.89	0.031	0.1	0.78	2.6
<b>CPD + C<sub>2</sub>H<sub>4</sub> (1 mol CPD / 1 mol C<sub>2</sub>H<sub>4</sub> / 10 mol N<sub>2</sub>)</b>						
973 K	5.3	0.12	0.004	3.1	0.01	8.3
1023 K	15.5	0.89	0.016	1.8	0.08	8.7
1073 K	35.8	6.29	0.028	0.4	0.34	5.4
1123 K	55.7	21.13	0.019	0.1	0.35	1.7
1173 K	65.1	31.83	0.007	0.02	0.14	0.4

## Figures

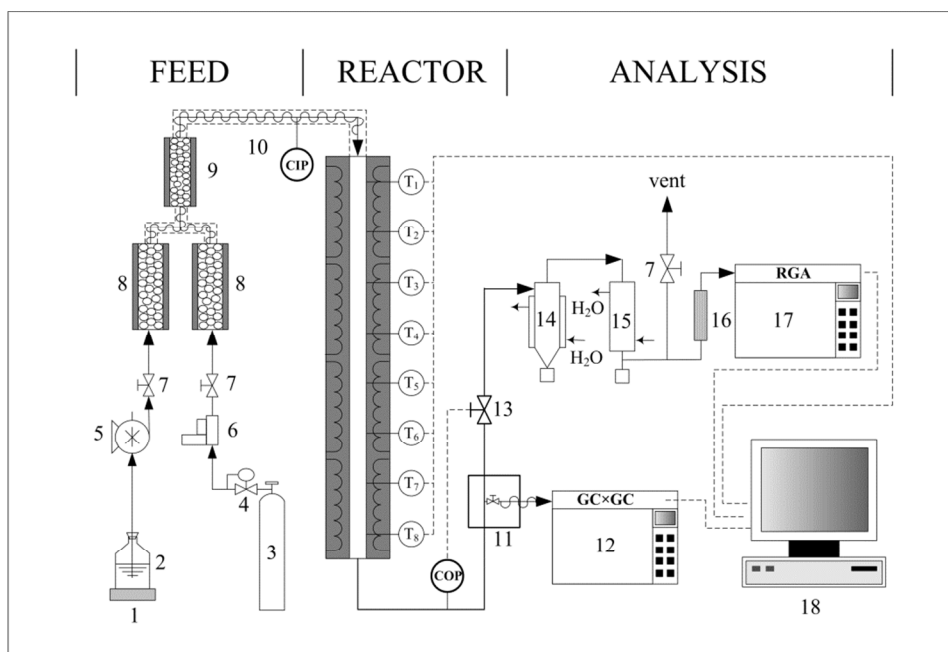


Figure S1. Schematic diagram of the experimental setup indicating process gas temperatures ( $T_i$ ) and pressure measurements (CIP & COP) (1-electronic balance; 2-liquid feed reservoir; 3-gaseous feed/diluent; 4-pressure reducing valve; 5-coriolis flow meter controlled pump; 6-coriolis mass flow controller; 7-valve; 8-evaporator/heater; 9-mixer; 10-heater; 11-heated sampling oven; 12-GC×GC-FID/TOF-MS for C5+; 13-outlet pressure restriction valve; 14-cyclone separator; 15-condenser; 16-dehydrator; 17-Refinery Gas Analyzer (RGA) for C4-; 18-data acquisition system).

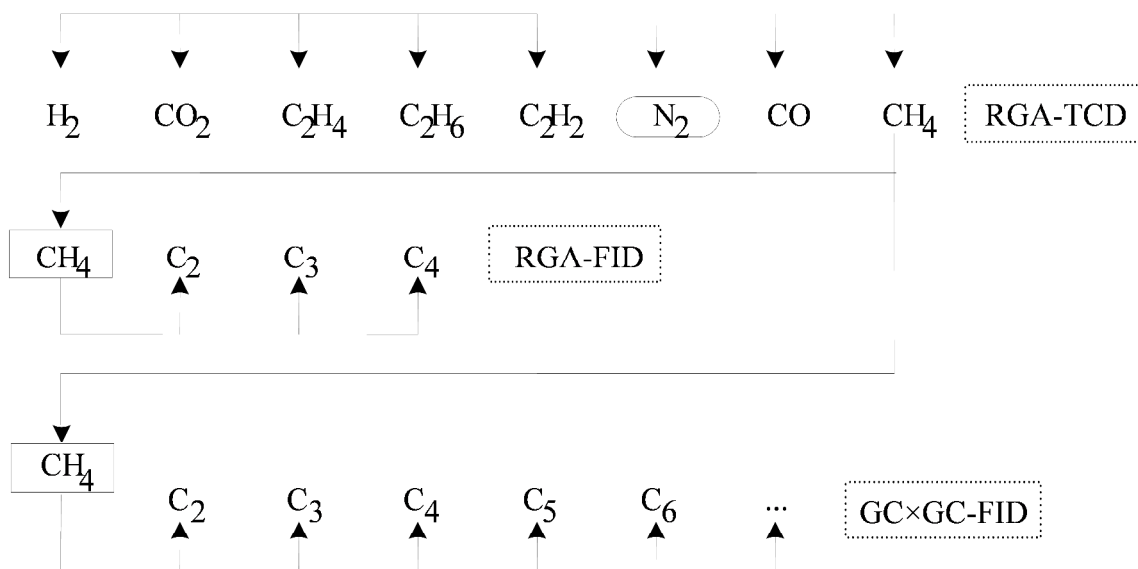


Figure S2. Use of the reference components in the product analysis section.

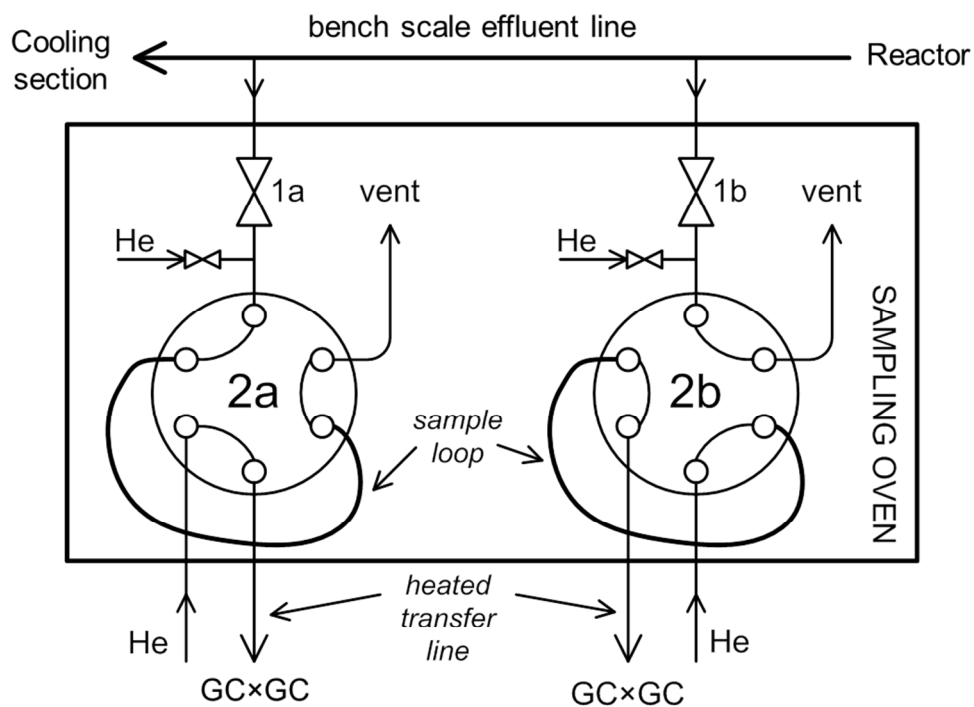


Figure S3. On-line effluent sampling system.

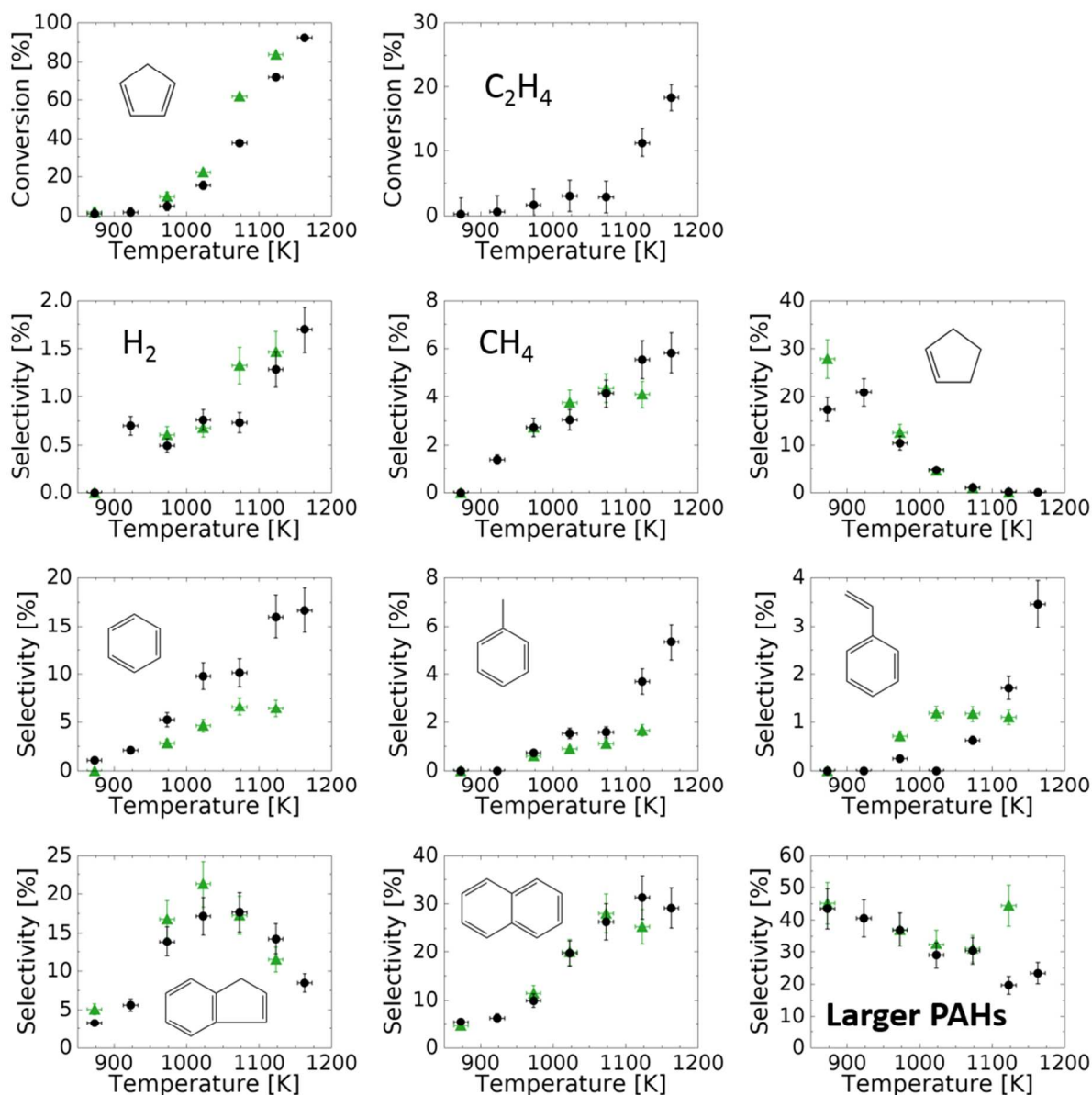


Figure S4. Experimentally determined conversion and selectivities of the major reaction products for the pyrolysis of cyclopentadiene<sup>8</sup> (green triangles, 0.17 MPa, dilution of 1 mol CPD / 5 mol N<sub>2</sub>, F<sub>0,CPD</sub> = 27 mg/s) and the co-pyrolysis of cyclopentadiene and ethene (black dots, 0.17 MPa, dilution 1 mol ethene / 1 mol CPD / 10 mol N<sub>2</sub>, F<sub>0,CPD</sub> = 13.6 mg/s).

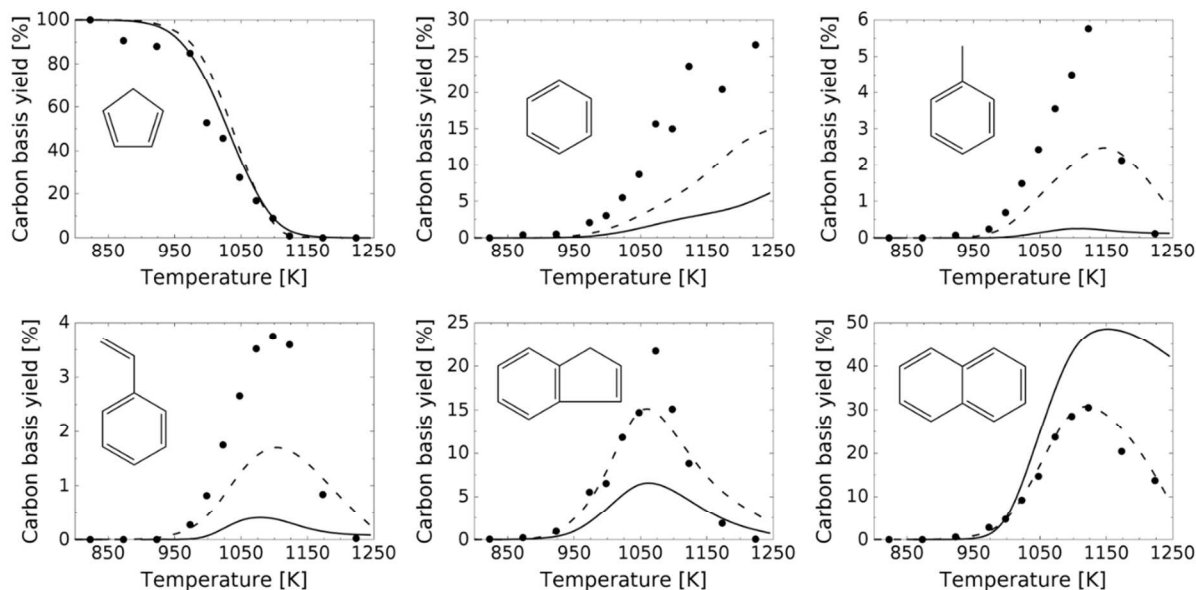


Figure S5. Experimental and simulated yields of the main reaction products during cyclopentadiene pyrolysis. Symbols: experimental data from Kim et al. <sup>6</sup> ( $[\text{CPD}]_0 = 0.7 \text{ mol\%}$ , nominal residence time 3 s), full lines: current model predictions, dashed lines: model predictions with the POLIMI\_1412 model.

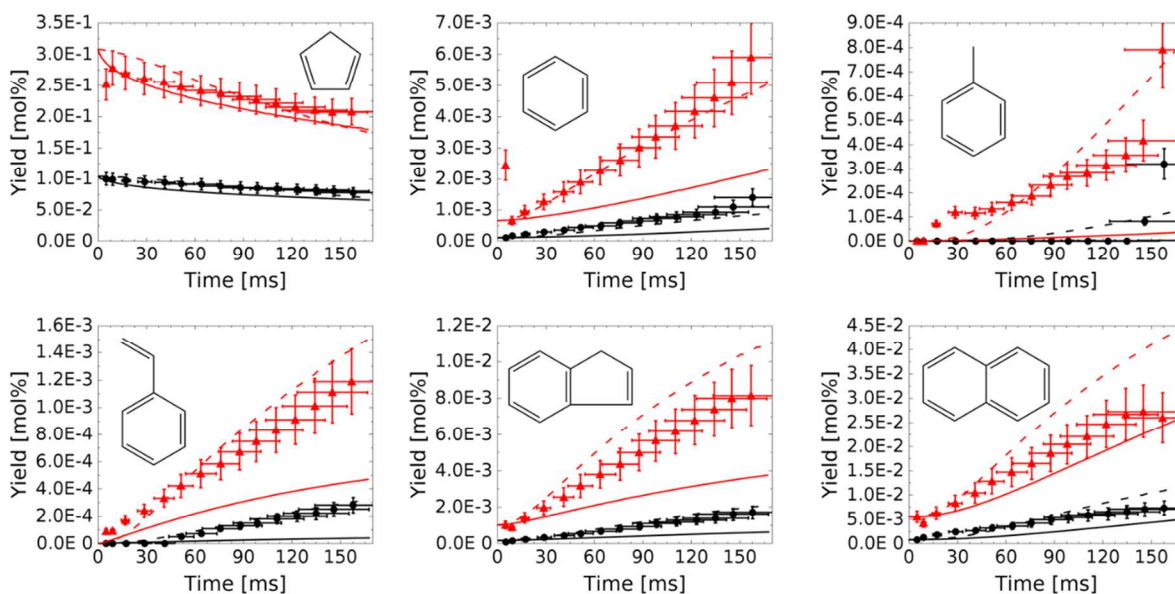


Figure S6. Experimental and simulated yields of the main reaction products during cyclopentadiene pyrolysis. Symbols: experimental data from Butler and Glassman <sup>13</sup>, Run 8

(black circles,  $\phi = 100$ ,  $T_0 = 1147$  K,  $[\text{CPD}]_0 = 2083$  ppmv), Run 10 (red triangles,  $\phi = 143$ ,  $T_0 = 1147$  K,  $[\text{CPD}]_0 = 3081$  ppmv). Full lines: current model predictions, dashed lines: model predictions with the POLIMI\_1412 model.

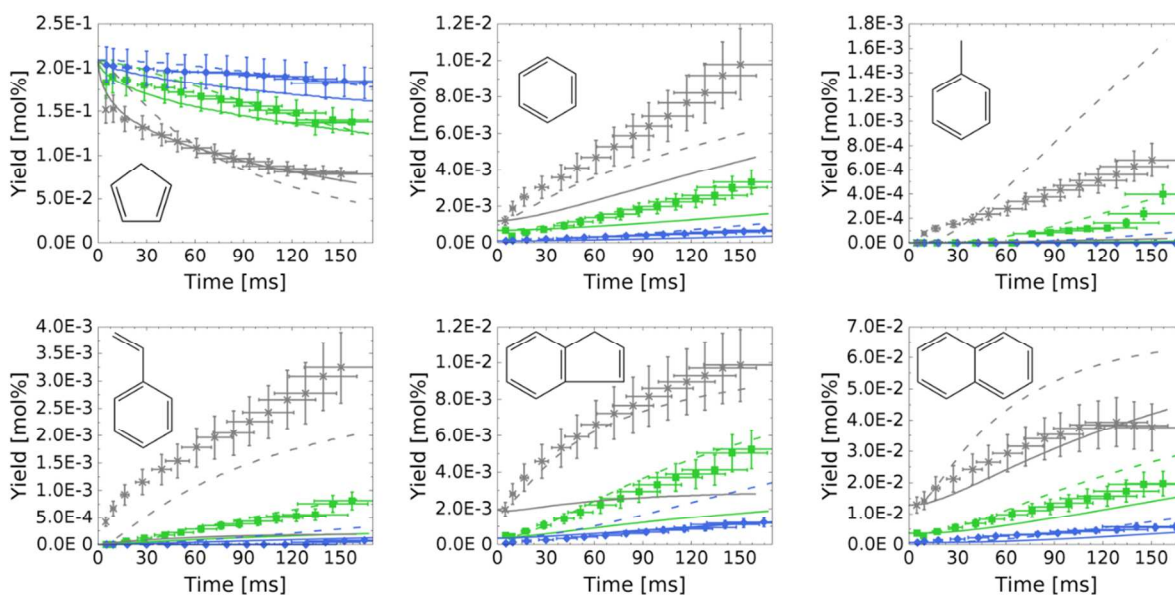


Figure S7. Experimental and simulated yields of the main reaction products during cyclopentadiene pyrolysis. Symbols: experimental data from Butler and Glassman<sup>13</sup>, Run 9 (green squares,  $\phi = 44.4$ ,  $T_0 = 1148$  K,  $[\text{CPD}]_0 = 1044$  ppmv), Run 11 (blue diamonds,  $\phi = 98.6$ ,  $T_0 = 1106$  K,  $[\text{CPD}]_0 = 2094$  ppmv), Run 12 (gray crosses,  $\phi = 97.8$ ,  $T_0 = 1202$  K,  $[\text{CPD}]_0 = 2077$  ppmv). Full lines: current model predictions, dashed lines: model predictions with the POLIMI\_1412 model.

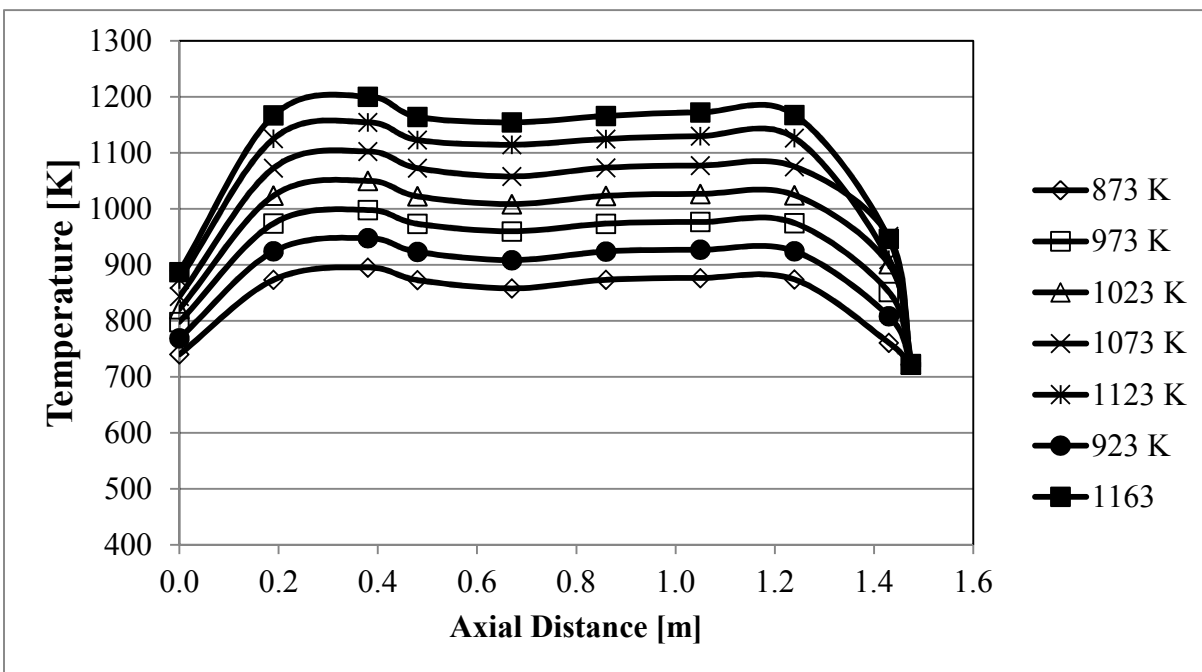


Figure S8. Axial temperature profiles of the tubular continuous flow reactor.



## References

1. Van Geem, K. M.; Pyl, S. P.; Marin, G. B.; Harper, M. R.; Green, W. H., Accurate High-Temperature Reaction Networks for Alternative Fuels: Butanol Isomers. *Industrial & Engineering Chemistry Research* **2010**, 49, (21), 10399-10420.
2. Harper, M. R.; Van Geem, K. M.; Pyl, S. P.; Marin, G. B.; Green, W. H., Comprehensive reaction mechanism for n-butanol pyrolysis and combustion. *Combustion and Flame* **2011**, 158, (1), 16-41.
3. Pyl, S. P.; Schietekat, C. M.; Van Geem, K. M.; Reyniers, M.-F.; Vercammen, J.; Beens, J.; Marin, G. B., Rapeseed oil methyl ester pyrolysis: On-line product analysis using comprehensive two-dimensional gas chromatography. *Journal of Chromatography A* **2011**, 1218, (21), 3217-3223.
4. Pyl, S. P.; Van Geem, K. M.; Puimège, P.; Sabbe, M. K.; Reyniers, M.-F.; Marin, G. B., A comprehensive study of methyl decanoate pyrolysis. *Energy* **2012**, 43, (1), 146-160.
5. Djokic, M.; Carstensen, H.-H.; Van Geem, K. M.; Marin, G. B., The thermal decomposition of 2,5-dimethylfuran. *Proceedings of the Combustion Institute* **2013**, 34, (1), 251-258.
6. Kim, D. H.; Mulholland, J. A.; Wang, D.; Violi, A., Pyrolytic Hydrocarbon Growth from Cyclopentadiene. *The Journal of Physical Chemistry A* **2010**, 114, (47), 12411-12416.
7. Nakos, J. T. *Uncertainty Analysis of Thermocouple Measurements Used in Normal and Abnormal Thermal Environment Experiments at Sandia's Radiant Heat Facility and Lurance Canyon Burn Site*; Sandia National Laboratories: 2004.
8. Djokic, M. R.; Van Geem, K. M.; Cavallotti, C.; Frassoldati, A.; Ranzi, E.; Marin, G. B., An experimental and kinetic modeling study of cyclopentadiene pyrolysis: First growth of polycyclic aromatic hydrocarbons. *Combustion and Flame* **2014**, 161, (11), 2739-2751.
9. Geem, K. M. V.; Dhuyvetter, I.; Prokopiev, S.; Reyniers, M.-F. o.; Viennet, D.; Marin, G. B., Coke Formation in the Transfer Line Exchanger during Steam Cracking of Hydrocarbons. *Industrial & Engineering Chemistry Research* **2009**, 48, (23), 10343-10358.
10. Beens, J.; Boelens, H.; Tijssen, R.; Blomberg, J., Quantitative Aspects of Comprehensive Two-Dimensional Gas Chromatography (GC×GC). *Journal of High Resolution Chromatography* **1998**, 21, (1), 47-54.
11. Roy, K.; Braun-Unkhoff, M.; Frank, P.; Just, T., Kinetics of the cyclopentadiene decay and the recombination of cyclopentadienyl radicals with H-atoms: Enthalpy of formation of the cyclopentadienyl radical. *International Journal of Chemical Kinetics* **2001**, 33, (12), 821-833.
12. Long, A. E.; Merchant, S. S.; Vandeputte, A. G.; Carstensen, H.-H.; Vervust, A. J.; Marin, G. B.; Van Geem, K. M.; Green, W. H., Pressure dependent kinetic analysis of pathways to naphthalene from cyclopentadienyl recombination. *Combustion and Flame* **2018**, 187, 247-256.
13. Butler, R. G.; Glassman, I., Cyclopentadiene combustion in a plug flow reactor near 1150K. *Proceedings of the Combustion Institute* **2009**, 32, (1), 395-402.